VIP *Very Important Paper*

Protein-Protein Recognition Involved in the Intermodular Transacylation Reaction in Modular Polyketide Synthase in the Biosynthesis of Vicenistatin

Taichi Chisuga,[a] Akimasa Miyanaga,*[a] and Tadashi Eguchi*[a]

The ketosynthase (KS) domain is a core domain found in modular polyketide synthases (PKSs). To maintain the polyketide biosynthetic fidelity, the KS domain must only accept an acyl group from the acyl carrier protein (ACP) domain of the immediate upstream module even when they are separated into different polypeptides. Although it was reported that both the docking domain-based interactions and KS-ACP compatibility are important for the interpolypeptide transacylation reaction in 6-deoxyerythronolide B synthase, it is not clear whether these findings are broadly applied to other modular PKSs. Herein, we describe the importance of protein-protein recognition in the intermodular transacylation between VinP1 module 3 and VinP2 module 4 in vicenistatin biosynthesis. We compared the transacylation activity and crosslinking efficiency of VinP2 KS_4 against the cognate VinP1 ACP_3 with the non-cognate one. As a result, it appeared that VinP2 KS_4 distinguishes the cognate ACP_3 from other ACPs.

Introduction

Polyketide synthases (PKSs) are responsible for the biosynthesis of various structurally diverse bioactive polyketide natural products.[1] Bacterial modular type I PKSs are huge multifunctional proteins, and are comprised of multiple modules, each of which contains a set of catalytic domains for one round of polyketide chain elongation.[2] Ketosynthase (KS), acyltransferase (AT), and acyl carrier protein (ACP) domains are essential for the polyketide chain elongation in each module. In the polyketide chain elongation in the Nth module, the AT domain (AT_N) transfers a specific malonyl-type extender unit onto the terminal thiol group of the phosphopantetheine arm of the ACP_N. KS_N receives the growing polyketide chain on the thiol group of the catalytic Cys residue from the ACP domain (ACP_{N-1}) of the upstream N-1th module, and subsequently catalyzes a decarboxylative Claisen-like condensation with the malonyl-type extender unit on ACP_N to afford β-ketoacyl-ACP_N (Figure 1). This β-ketoacyl-group is optionally modified by reduction and dehydration reactions catalyzed by other catalytic domains thus completing the polyketide chain elongation in the Nth module. The acyl group on ACP_N is transferred to KS_{N+1}, which initiates the polyketide chain elongation in the N+1th module. To maintain the structural integrity of the polyketide products, the growing polyketide chain must be transferred between modules in the correct order.

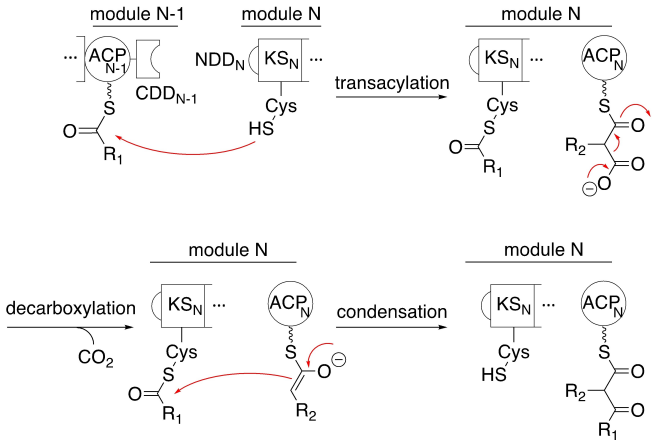

Figure 1. Proposed reaction mechanism of the type I PKS KS domain.

For the functional intermodular transacylation reaction of the KS_N domain, KS_N must only accept an acyl group from the ACP_{N-1} domain of the immediate upstream module. When KS_N and ACP_{N-1} are separated into different polypeptides, complementary short linker regions referred to as docking domains (DDs) located at the N-terminus of KS_N and C-terminus of ACP_{N-1} (called NDD_N and CDD_{N-1}, respectively) have been shown to mediate the functional intermodular transacylation reaction between polypeptides.[3] Several studies show that docking domain compatibility is essential to maintain the biosynthetic fidelity in the intermodular transacylation reaction between polypeptides in bacterial *cis*-AT PKSs.[4–7] The protein-protein recognition between KS_N and ACP_{N-1} was also reported to be important in the intermodular transacylation reaction between polypeptides in 6-deoxyerythronolide B synthase (DEBS).[8,9] However, studies on the KS_N-ACP_{N-1} interactions between

[a] *T. Chisuga, Dr. A. Miyanaga, Prof. Dr. T. Eguchi*
Department of Chemistry
Tokyo Institute of Technology, 2-12-1 O-okayama
Meguro-ku, Tokyo 152-8551 (Japan)
E-mail: miyanaga.a.aa@m.titech.ac.jp
eguchi@chem.titech.ac.jp

Supporting information for this article is available on the WWW under https://doi.org/10.1002/cbic.202200200

© 2022 The Authors. ChemBioChem published by Wiley-VCH GmbH. This is an open access article under the terms of the Creative Commons Attribution Non-Commercial NoDerivs License, which permits use and distribution in any medium, provided the original work is properly cited, the use is non-commercial and no modifications or adaptations are made.

© 2022 The Authors. ChemBioChem published by Wiley-VCH GmbH

polypeptides have been limited to DEBS among the bacterial *cis*-AT PKSs. Therefore, it is necessary to investigate whether the findings on selective KS_N-ACP_{N-1} interactions are broadly applicable to other modular type I *cis*-AT PKSs to better understand the molecular basis of intermodular transacylation reactions in modular type I *cis*-AT PKSs.

In this study, we performed in vitro analysis of the intermodular transacylation reaction between VinP1 module 3 (UniProt; Q76KY0) and VinP2 module 4 (UniProt; Q76KZ5) from the macrolactam antibiotic vicenistatin PKS[10] to gain insights into protein-protein recognition in the intermodular transacylation reaction between the polypeptides.

Results and Discussion

The intermodular transacylation reaction between VinP1 module 3 and VinP2 module 4

To determine the importance of protein-protein recognition in the intermodular transacylation reaction in which the modules are separated into different polypeptides, we attempted to analyze the transacylation reaction from acyl-$ACP_{N-1}CDD_{N-1}$ to NDD_NKS_N. We selected the VinP2 KS_4 domain ($_4$; in module 4) (Pro35-Pro461), which is predicted to accept a polyketide intermediate from the upstream module 3 in vicenistatin biosynthesis (Figure 2A).[10] Module 3 and module 4 of vicenistatin PKS are separated into VinP1 and VinP2, respectively, and the docking domains are located at the C-terminus of VinP1 (CDD_3; Asp5813-Leu5823) and at the N-terminus of VinP2 (NDD_4; Met1-Glu34) (Figure S1). VinP1 CDD_3 and VinP2 NDD_4 belong to class 1 docking domains[3] and have high amino acid sequence similarities with the structurally characterized DEBS2 CDD_4 and DEBS3 NDD_5 at 55% and 50%, respectively (Figure S2). We expected that in vitro analysis of the transacylation reaction of the VinP2 KS_4 domain is suitable for evaluation of the protein-protein recognition involved in the intermodular transacylation reaction between polypeptides. We expressed recombinant VinP2 NDD_4KS_4 protein that contained the neighboring AT_4 domain (Met1-Gly931) in *Escherichia coli* because it was reported that type I PKS KS recombinant protein expressed as a single domain is often obtained as an insoluble form.[11,12] To exclude the effect of the VinP2 AT_4 domain, we prepared the VinP2 $NDD_4KS_4AT_4$ S684G mutant in which the catalytic Ser684 residue of the AT_4 domain was mutated. We also expressed recombinant VinP1 ACP_3CDD_3 protein (Asp5651-Asp5826) (Figure S3) in *E. coli*. We prepared tiglyl- and butyryl-VinP1 ACP_3CDD_3 (Figures 2B, S4A) as simplified mimics of the native substrate for the VinP2 KS_4 domain (Figure 2A) by the enzymatic reaction of phosphopantetheinyl transferase Sfp[13] with VinP1 ACP_3CDD_3 in the presence of tiglyl-CoA and butyryl-CoA, respectively (Figure S5).

We performed the transacylation reaction of VinP2 NDD_4KS_4 by mixing 50 μM of VinP2 $NDD_4KS_4AT_4$ S684G and 50 μM of tiglyl- or butyryl-VinP1 ACP_3CDD_3, and analyzed the reaction products by high-performance liquid chromatography (HPLC). As a result, both tiglyl- and butyryl-VinP1 ACP_3CDD_3 were consumed, and holo-VinP1 ACP_3CDD_3 was produced by the transacylation reaction (Figure 2C, D, Figures S4B, S6A). By comparison, in the reaction with VinP2 $NDD_4KS_4AT_4$ C206G/S684G in which the catalytic Cys206 of the KS_4 domain was mutated (Figure S7A), the consumption of tiglyl- and butyryl-VinP1 ACP_3CDD_3 was almost undetectable (Figures 2D, S4B). These results showed that the transacylation reaction from VinP1 ACP_3CDD_3 to VinP2 NDD_4KS_4 occurs on the catalytic Cys206 of the KS_4 domain. VinP2 NDD_4KS_4 showed similar activities against tiglyl- and butyryl-VinP1 ACP_3CDD_3 (Table S1), suggesting that the VinP2 KS_4 domain is tolerant to hydrophobic acyl groups at the α and β positions. We selected tiglyl-VinP1 ACP_3CDD_3 for further analysis because the tiglyl group is more similar to the native polyketide intermediate for the transacylation reaction of the VinP2 KS_4 domain.

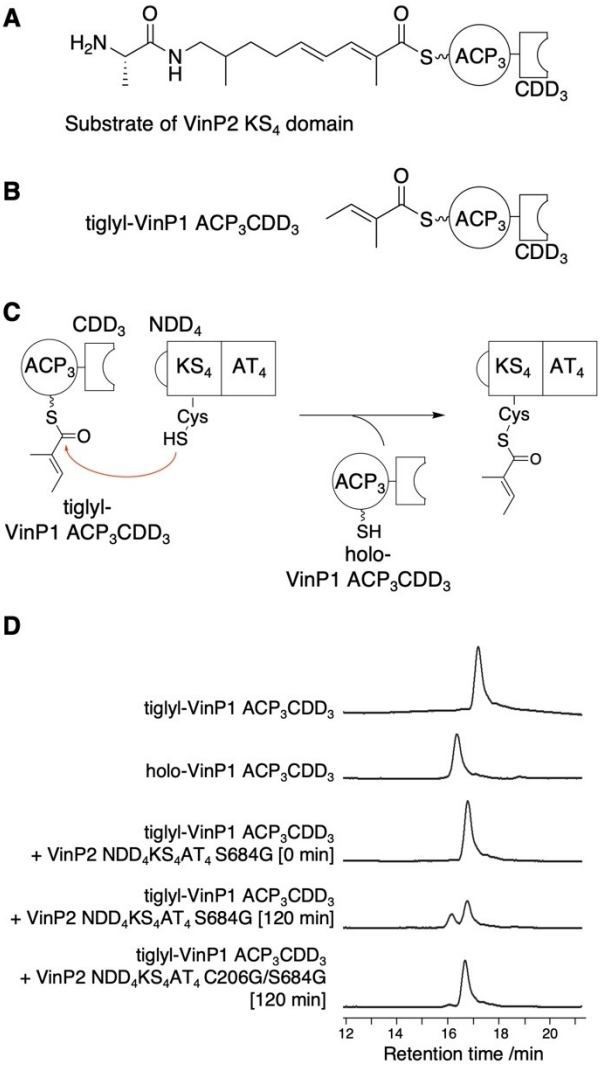

Figure 2. Transacylation reaction between the VinP2 NDD_4KS_4 domain and VinP1 ACP_3CDD_3. A) The substrate of the VinP2 KS_4 domain. B) Tiglyl-ACP_3CDD_3, which is a substrate mimic for the VinP2 KS_4 domain. C) The transacylation reaction between tiglyl-VinP1 ACP_3CDD_3 and VinP2 $NDD_4KS_4AT_4$ S684G. D) HPLC analysis of the transacylation reaction between the VinP2 NDD_4KS_4 domain and VinP1 ACP_3CDD_3.

© 2022 The Authors. ChemBioChem published by Wiley-VCH GmbH

The KS domains of PKSs have two conserved His residues located near the catalytic Cys residue (Figure S7A, B). Using the in vitro analytical system of the VinP2 NDD_4KS_4 domain, we performed mutational analysis of the two conserved His residues (His341 and His381) of the VinP2 KS_4 domain. As a result, VinP2 KS_4AT_4 H341A/S684G and H381A/S684G showed significantly reduced transacylation activity (Figures S7A, S8, Table S2), which is consistent with previous mutational analysis of the DEBS1 KS_1 domain.[14] These results suggest that the two conserved His residues are important for the transacylation reaction (Figure S9).

The protein-protein recognition between VinP2 NDD_4KS_4 and ACPCDD in the transacylation reaction

In vicenistatin biosynthesis, VinP2 ACP_4CDD_4 and VinP3 ACP_6CDD_6 are also involved in the intermodular transacylation reaction between polypeptides in addition to VinP1 ACP_3CDD_3 (Figure S1). VinP2 NDD_4KS_4 must only accept an acyl substrate from VinP1 ACP_3CDD_3 to maintain the biosynthetic fidelity. To confirm that VinP2 NDD_4KS_4 can distinguish VinP1 ACP_3CDD_3 from other ACPCDDs, we carried out the transacylation reaction using tiglyl-VinP2 ACP_4CDD_4 and tiglyl-VinP3 ACP_6CDD_6, respectively (Figures S10, S11). As expected, the formation of holo-VinP2 ACP_4CDD_4 and holo-VinP3 ACP_6CDD_6 was not detected (Table 1, Figure S12), implying that VinP2 NDD_4KS_4 does not accept an acyl group from VinP2 ACP_4CDD_4 or VinP3 ACP_6CDD_6. Thus, the exchange of ACPCDD resulted in a significant decrease in the transacylation activity of VinP2 NDD_4KS_4 (Table 1), confirming that the protein-protein recognition between ACP_3CDD_3 and NDD_4KS_4 is important for the intermodular transacylation reaction between VinP1 and VinP2.

Next, we assessed the importance of the ACP and CDD parts for the transacylation reaction of VinP2 NDD_4KS_4. First, we evaluated the effect of the CDD part on the transacylation reaction of VinP2 NDD_4KS_4. VinP1 ACP_3CDD_3 has a post-ACP dimerization element (DE) region, which promotes dimerization of an ACPCDD protein, between the ACP domain and CDD as reported for other class 1 DDs (Figure S3A, B).[6] To assess the effect of the CDD part only, we prepared VinP1 ACP_3DE_3 (Asp5651-Gln5798), from which CDD_3 (Asp5813-Asp5826) was removed, and then performed the transacylation reaction of VinP2 NDD_4KS_4 with tiglyl-VinP1 ACP_3DE_3 (Figure S13). As a result, VinP2 NDD_4KS_4 showed a significantly reduced activity against tiglyl-VinP1 ACP_3DE_3 (Table 1, Figure S14), indicating that the CDD_3 part is very important for protein-protein recognition in the transacylation reaction of VinP2 NDD_4KS_4. The interactions between VinP1 CDD_3 and VinP2 NDD_4 are presumed to be formed by the interaction of the hydrophobic surface and two salt bridges as observed for DEBS2 CDD_4 and DEBS3 NDD_5, between which the detailed interface interaction was previously elucidated by NMR spectroscopy analysis[6] (Figure S2C).

Table 1. Initial velocity of the transacylation reaction between the VinP2 NDD_4KS_4 domain and the tiglyl-ACPCDD proteins.

ACP part	CDD part	Initial velocity [nM/min][a]
ACP3	CDD3	436 ± 34
ACP3	none	trace[b]
ACP4	CDD4	trace
ACP6	CDD6	trace
ACP4	CDD3	76.2 ± 5.0
ACP6	CDD3	10.5 ± 2.2
ACP7	CDD3	15.7 ± 1.3

[a] Initial velocity of 50 μM VinP2 $NDD_4KS_4AT_4$ S684G and 50 μM tiglyl-ACPCDD. [b] Initial velocity < 10 nM/min.

To evaluate the importance of the ACP part for the protein-protein recognition in the transacylation reaction of VinP2 NDD_4KS_4, we designed chimeric ACP_xCDD_3 proteins (x; module number) in which the ACP_3 part of VinP1 ACP_3CDD_3 was replaced with other ACP domains. We fused the ACP domain of another module with the N-terminus of the VinP1 DE_3CDD_3 part (Glu5747-Asp5826) to generate the chimeric ACP_xCDD_3 proteins ACP_4CDD_3, ACP_6CDD_3 and ACP_7CDD_3 (Figures S15–S19). We then performed the transacylation reaction of VinP2 NDD_4KS_4 with the tiglyl-chimeric ACP_xCDD_3 protein (Figures S20-S22). The results showed that the activities against all chimeric ACP_xCDD_3 proteins were greatly reduced compared to that against cognate VinP1 ACP_3CDD_3 (Table 1, Figure S23). Interestingly, VinP2 NDD_4KS_4 showed relatively high activity against tiglyl-ACP_4CDD_3, among the tiglyl-chimeric ACP_xCDD_3 proteins. Previous studies of the type I PKS KS domain suggested that the binding mode of the upstream module ACP_{N-1} to the KS_N domain is different from that of the same module ACP_N.[15,16] The VinP2 ACP_4 domain interacts with the VinP2 KS_4 domain to provide a methylmalonyl extender unit during the Claisen-like condensation reaction. Therefore, the VinP2 KS_4 domain might be able to interact with the tiglyl-VinP2 ACP_4 domain in a binding mode suitable for condensation although the binding mode of the VinP1 ACP_4 domain is less favorable for the transacylation reaction than that of the VinP1 ACP_3 domain. Comparison of the transacylation activities against these chimeric ACP_xCDD_3 proteins revealed that the ACP moiety is also important for the transacylation reaction of VinP2 NDD_4KS_4.

Evaluation of the protein-protein recognition between VinP2 NDD_4KS_4 and ACPCDDs by the crosslinking reaction

Comparison of the transacylation activities showed that the protein-protein recognition of both the VinP1 ACP_3-VinP2 KS_4 domain and VinP1 CDD_3-VinP2 NDD_4 are important for the intermodular transacylation reaction between the VinP1 module 3 and VinP2 module 4. To further evaluate the protein-protein recognition between the VinP2 NDD_4KS_4 and ACPCDD proteins, we performed another assay using crosslinking probes. Recently, many crosslinking probes have been used as chemical tools to enable structural and functional characterization of the transient interactions between the catalytic domains and ACP domains in PKS and fatty acid synthase.[17–23] Therefore, we investigated the efficiencies of crosslinking between the VinP2 NDD_4KS_4 and ACPCDD proteins to compare with the results of

© 2022 The Authors. ChemBioChem published by Wiley-VCH GmbH

the analysis of the transacylation reaction. To crosslink the VinP2 NDD_4KS_4 and ACPCDD proteins, we used Br-acetyl pantetheinamide and Cl-acetyl pantetheinamide, both of which are phosphopantetheine analogs that have electrophilic reactive groups at their terminus.[20,24–26] We prepared *crypto*-VinP1 ACP_3CDD_3, which is VinP1 ACP_3CDD_3 modified with α-haloacyl-pantetheinamides using CoA biosynthetic enzymes (CoaA, CoaD and CoaE) and Sfp (Figure S5).[27] The thiol group of the Cys206 catalytic residue of the VinP2 KS_4 domain was expected to participate in a nucleophilic attack on the α-haloacyl-pantetheinamide moiety on the *crypto*-ACPCDD protein to form a covalent bond (Figure 3A). We performed the crosslinking reaction by mixing 200 μM *crypto*-VinP1 ACP_3CDD_3 and 50 μM VinP2 $NDD_4KS_4AT_4$ S684G, and then analyzed the crosslinking efficiency by SDS-PAGE (Figures 3B, S24). The crosslinking reaction using Br-acetyl pantetheiamide-VinP1 ACP_3CDD_3 gave several crosslinked complexes, while the crosslinking reaction using Cl-acetyl pantetheiamide-VinP1 ACP_3CDD_3 gave a single crosslinked complex (Figures 3B, S24). In the case of VinP2 $NDD_4KS_4AT_4$ C206G/S684G, the reaction with Br-acetyl pantetheiamide-VinP1 ACP_3CDD_3 resulted in the formation of the crosslinked complex. These observations suggest that the Br-acetoamide group is too reactive toward VinP2 $NDD_4KS_4AT_4$, resulting in the formation of undesired crosslinked complexes via other nucleophilic residues as reported for the VinK-VinL crosslinking reaction.[28] By comparison, in the crosslinking reaction of VinP2 $NDD_4KS_4AT_4$ C206G/S684G using Cl-acetyl pantetheiamide-VinP1 ACP_3CDD_3, almost no crosslinked complex was generated. Thus, Cl-acetyl pantetheinamide-VinP1 ACP_3CDD_3 only reacts with the Cys206 catalytic residue, and seems to be suitable for the crosslinking reaction between VinP2 NDD_4KS_4 and VinP1 ACP_3CDD_3.

Next, we compared the efficiency of the crosslinking reaction of the VinP2 KS_4 domain with cognate ACP_3 and noncognate ACP proteins. Cl-Acetyl pantetheinamide was used to prepare each *crypto*-ACP protein in the same manner as *crypto*-VinP1 ACP_3CDD_3. We mixed 50 μM VinP2 $NDD_4KS_4AT_4$ S684G with 200 μM *crypto*-ACP protein, and quantified the amount of crosslinked complexes using SDS-PAGE (Figure 3C, Table S3). The amount of the crosslinked complex with ACP_3DE_3 was much lower than that with VinP1 ACP_3CDD_3, confirming the importance of the docking domain in the crosslinking reaction between the VinP2 KS_4 domain and ACP_3DE_3 (Table S3). The crosslinking reaction with ACP_4CDD_4 and ACP_6CDD_6 gave almost no crosslinked complex. The crosslinking reaction using chimeric ACP_xCDD_3 proteins also resulted in a substantial decrease in the amount of the crosslinked complex, except for a modest decrease in the case of ACP_4CDD_3. These crosslinking reaction results are consistent with those of the transacylation reaction (Table 1, S3).

Conclusion

In this study, we investigated the protein-protein recognition involved in the intermolecular transacylation reaction between VinP1 ACP_3CDD_3 and VinP2 NDD_4KS_4 in vicenistatin PKS. It was found that both the VinP1 CDD_3 and ACP_3 parts are important for the transacylation activity of VinP2 NDD_4KS_4. Furthermore, the substitution of the VinP1 ACP_3 part with other ACP domains

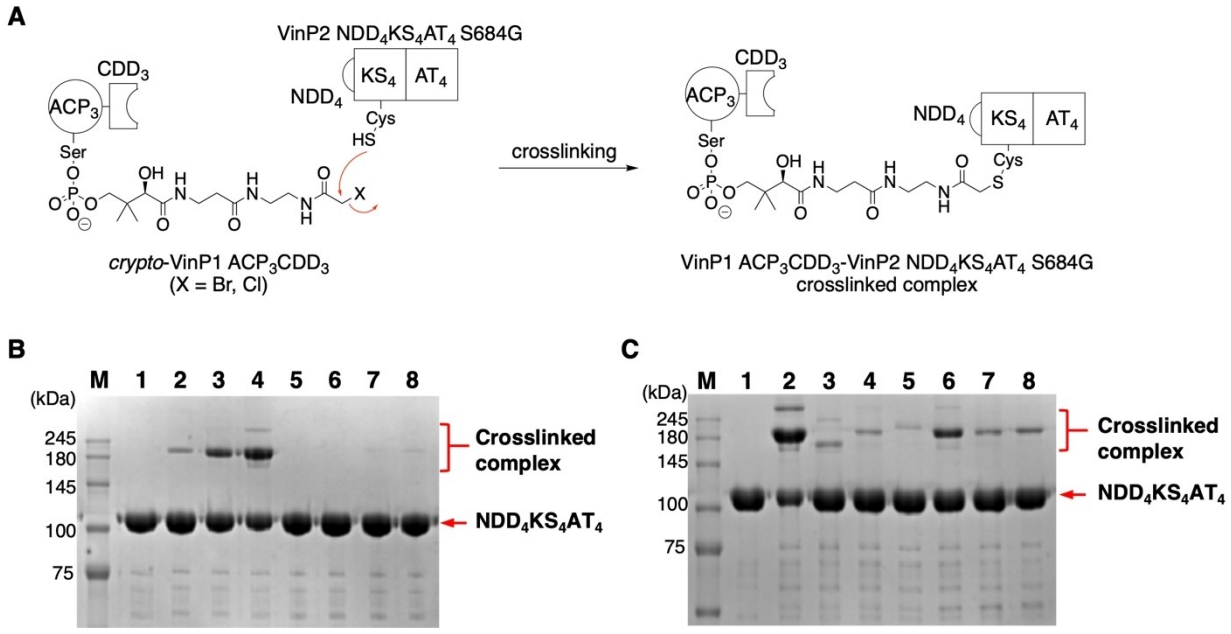

Figure 3. A) Crosslinking between VinP2 $NDD_4KS_4AT_4$ S684G and *crypto*-VinP1 ACP_3CDD_3. B) SDS-PAGE analysis of the crosslinking reaction with Cl-acetyl pantetheinamide-ACP_3CDD_3. Lane M: Protein Marker. Lanes 1–4: crosslinking reaction of VinP2 $NDD_4KS_4AT_4$ S684G at 0, 15, 120 and 360 min reaction times, respectively. Lanes 5–8: crosslinking reaction of VinP2 $NDD_4KS_4AT_4$ C206G/S684G at 0, 15, 120 and 360 min reaction times, respectively. C) Crosslinking reaction of VinP2 $NDD_4KS_4AT_4$ S684G with various *crypto*-ACP proteins. Lane M: Protein Marker. Lane 1: without *crypto*-ACP. Lane 2: with *crypto*-ACP_3CDD_3. Lane 3: with *crypto*-ACP_3. Lane 4: with *crypto*-ACP_4CDD_4. Lane 5: with *crypto*-ACP_6CDD_6. Lane 6: with *crypto*-ACP_4CDD_3. Lane 7: with *crypto*-ACP_6CDD_3. Lane 8: with *crypto*-ACP_7CDD_3.

© 2022 The Authors. ChemBioChem published by Wiley-VCH GmbH

resulted in significantly reduced crosslinking efficiency between ACPCDD and VinP2 NDD_4KS_4. These results suggest the importance of the protein-protein recognition between VinP2 NDD_4KS_4 and VinP1 ACP_3CDD_3 in the intermodular transacylation reaction. The protein-protein recognition mechanism between the NDD and CDD of *cis*-AT PKSs involved in the intermodular transacylation reactions between polypeptides has been elucidated in detail based on structural analysis.[6,7,29] However, the protein-protein recognition mechanism between the KS domain and the upstream ACP of type I PKSs is not fully understood although the results from various in vitro experiments and low-resolution cryo-electron microscopy analysis have successfully identified the regions of ACP involved in the protein-protein recognition between the KS domain and the upstream ACP.[8,9,15,30,31] A high-resolution structure of a type I PKS KS domain complexed with the upstream ACP is necessary to fully understand the protein-protein recognition mechanism between the KS domain and the upstream ACP in the intermodular transacylation reaction.

Experimental Section

Preparation of the VinP2 $NDD_4KS_4AT_4$ protein, VinP1 ACP_3CDD_3, VinP1 ACP_3 domain and chimeric ACP_xCDD_3 proteins: The *vinP2 $NDD_4KS_4AT_4$* fragment was amplified by PCR using cosmid K1B10[10] as the template DNA with the oligonucleotides shown in Table S4. The amplified fragment was cloned into the expression vector pET30 (Novagen) using *Nde*I and *Eco*RI restriction sites to form pET30-*vinP2 $NDD_4KS_4AT_4$*. For preparation of pET30-*vinP2 $NDD_4KS_4AT_4$* S684G, site-directed mutagenesis was performed using pET30-*vinP2 $NDD_4KS_4AT_4$* as the template DNA with the oligonucleotides shown in Table S4. For preparation of pET30-*vinP2 $NDD_4KS_4AT_4$* C206G/S684G, site-directed mutagenesis was performed using pET30-*vinP2 $NDD_4KS_4AT_4$* S684G as the template DNA with the oligonucleotides shown in Table S4. These plasmids were transformed into *E. coli* Rosetta™ 2(DE3) (Novagen).

For the expression of the VinP2 $NDD_4KS_4AT_4$ protein, *E. coli* Rosetta™ 2(DE3) cells harboring pET30-*vinP2 $NDD_4KS_4AT_4$* were grown at 37 °C in Luria-Bertani (LB) broth containing kanamycin (50 μg/mL) and chloramphenicol (20 μg/mL). When the optical density at 600 nm reached 0.6, protein expression was induced by the addition of 0.2 mM isopropyl β-D-1-thiogalactopyranoside (IPTG), and the cells were then cultured for an additional 20 h at 15 °C. The harvested cell pellets were suspended in buffer A [50 mM HEPES–Na (pH 8.0), 100 mM NaCl, and 10% (w/v) glycerol] and lysed by sonication. The recombinant VinP2 $NDD_4KS_4AT_4$ protein was purified from the lysate using a His60 Ni Superflow affinity column (Clontech). The protein solution was then desalted and concentrated using a PD-10 column (Cytiva) and an Amicon Ultra 10 K centrifugal filter (Merck Millipore). The VinP2 $NDD_4KS_4AT_4$ S684G mutant and C206G/S684G double mutant were also prepared as described above.

The *vinP1 ACP_3CDD_3* fragment was amplified by PCR using cosmid K1B10 as the template DNA with the oligonucleotides shown in Table S5. The amplified fragment was cloned into the expression vector pColdW (modified vector derived from pColdI)[12] using *Nde*I and *Xho*I restriction sites to form pColdW-*vinP1 ACP_3CDD_3*. For the expression of the VinP1 ACP_3CDD_3, *E. coli* BL21(DE3) (Nippon Gene Co., Ltd.) cells harboring pColdW-*vinP1 ACP_3CDD_3* were grown at 37 °C in LB broth containing ampicillin (50 μg/mL). When the optical density at 600 nm reached 0.4, protein expression was induced by the addition of 0.2 mM IPTG, and the cells were then cultured for an additional 20 h at 15 °C. The harvested cell pellets were suspended in buffer A and lysed by sonication. The recombinant VinP1 ACP_3CDD_3 protein was purified from the lysate in the same manner as the VinP2 $NDD_4KS_4AT_4$ protein. The *vinP1 ACP_3DE_3* fragment was amplified by PCR using pColdW-*vinP1 ACP_3CDD_3* as the template DNA with the oligonucleotides shown in Table S5. The amplified fragment was cloned into the expression vector pColdW using *Nde*I and *Xho*I restriction sites to form pColdW-*vinP1 ACP_3DE_3*. Expression and purification of VinP1 ACP_3DE_3 were carried out using the same procedures as those for VinP1 ACP_3CDD_3.

The detailed methods for the construction of the plasmids encoding the chimeric ACP_xCDD_3 protein are described in the Supporting Information. Expression and purification of the chimeric ACP_xCDD_3 proteins were performed in the same manner as for VinP1 ACP_3CDD_3.

Preparation of holo- and acyl-ACP proteins: Tiglyl-VinP1 ACP_3CDD_3 was prepared by an enzymatic reaction using the phosphopantetheinyl transferase Sfp.[13] A total of 200 μM apo-VinP1 ACP_3CDD_3 in buffer A was mixed with 20 μM Sfp, 2 mM tiglyl-CoA and 5 mM $MgCl_2$, and then incubated at 28 °C for 10 min. After the reaction, the solution was directly used for the transacylation reaction assay. Preparation of holo- and butyryl-VinP1 ACP_3CDD_3 was performed in the same manner except for exchange of tiglyl-CoA with CoA and butyryl-CoA, respectively. Other holo- and tiglyl-ACP_xCDD_x proteins were prepared using the same procedure as holo- and tiglyl-VinP1 ACP_3CDD_3.

Analysis of the transacylation reaction between the VinP2 NDD_4KS_4 and acyl-ACPCDD proteins: For analysis of the transacylation reaction between VinP2 NDD_4KS_4 and tiglyl-VinP1 ACP_3CDD_3, 50 μM VinP2 $NDD_4KS_4AT_4$ S684G was mixed with 50 μM tiglyl-VinP1 ACP_3CDD_3 in buffer A. The reaction mixture was incubated at 28 °C for 8, 15, 30, 60, 120 and 240 min, and an equal volume of acetonitrile was then added to the solution. The mixtures were subjected to HPLC analysis using a Hitachi instrument (Chromaster Pump 5110, Diode Array Detector 5430, and Column Oven 5310) equipped with a Protein-R column (5 μm, 250× 4.6 mm^2; COSMOSIL) at 50 °C. Holo-VinP1 ACP_3CDD_3 was detected at 280 nm and eluted with a gradient of solvents B (0.1% TFA in water) and C (0.1% TFA in acetonitrile) at a flow rate of 1.5 mL/min (0–5 min 43% C, 5–25 min 43–53% C with a linear gradient, and 25–30 min 90% C) as a peak of retention time 16 min. The initial velocity of the transacylation between VinP2 NDD_4KS_4 and tiglyl-VinP1 ACP_3CDD_3 was calculated based on the HPLC peak area (Figure S6). Analyses of the transacylation between VinP2 NDD_4KS_4 and the other acyl-ACPCDD proteins were performed in the almost same manner except for the reaction time and the concentration of solvent C used in the HPLC analysis (Table S6).

Crosslinking reaction with α-haloacyl pantetheinamides: Br-Acetyl pantetheinamide and Cl-acetyl pantetheinamide were synthesized as described previously.[20] For the VinP2 $NDD_4KS_4AT_4$ S684G-*crypto*-ACP_3CDD_3 crosslinking reaction, *crypto*-ACP_3CDD_3 was prepared. A total of 600 μM of each α-haloacyl pantetheinamide was mixed with 5 mM ATP, 5 mM $MgCl_2$, 2 μM CoaA, 2.8 μM CoaD, 2.4 μM CoaE, 20 μM Sfp and 400 μM of apo-ACP_3CDD_3 protein in buffer A. This modified reaction was carried out at 28 °C for 3 h, and this reaction mixture was directly used for the crosslinking reaction. For the crosslinking reaction, 50 μM of VinP2 $NDD_4KS_4AT_4$ S684G (or VinP2 $NDD_4KS_4AT_4$ C206G/S684G) was mixed with 200 μM of *crypto*-ACP_3CDD_3, which was then incubated at 20 °C. At 15, 120 and 360 min, samples of the crosslinking reaction mixture were taken, and the reaction was quenched by the addition of an equal volume of SDS-PAGE loading buffer [1% (v/v) 2-mercaptoethanol, 20% (v/v) glycerol, 1% (w/w) sodium dodecyl sulfate, and 50 mM Tris-HCl

© 2022 The Authors. ChemBioChem published by Wiley-VCH GmbH

(pH 6.8)] and the samples were analyzed by SDS-PAGE. For the crosslinking reaction between the VinP2 $NDD_4KS_4AT_4$ S684G and Cl-acetyl pantetheinamide-ACP(CDD) proteins, 200 μM of Cl-acetyl pantetheinamide-ACP(CDD) protein that was prepared in the same manner as *crypto*-ACP_3CDD_3 was mixed with 50 μM of VinP2 $NDD_4KS_4AT_4$ S684G. After incubation at 20 °C for 15 h, samples of the crosslinking reaction mixture were taken, and the reaction was quenched by the addition of an equal volume of SDS-PAGE loading buffer. The amount of the crosslinked complex was calculated using a Gel Doc EZ Imager (software; Image Lab 4.0, BIO RAD).

Acknowledgements

This work was supported in part by Grants-in-Aid for Scientific Research (B) (20H02911 to A.M.) and Grants-in-Aid for JSPS Fellows (20J13080 to T.C.) from the Japan Society for the Promotion of Science, and Grants-in-Aid for Scientific Research on Innovative Areas (16H06451 to T.E.) from the Ministry of Education, Culture, Sports, Science, and Technology (MEXT).

Conflict of Interest

The authors declare no conflict of interest.

Data Availability Statement

The data that support the findings of this study are available from the corresponding author upon reasonable request.

Keywords: acyl carrier protein · biosynthesis · ketosynthases · polyketide synthases · protein-protein interactions

[1] C. T. Walsh, *Science* **2004**, *303*, 1805–1810.
[2] A. T. Keatinge-Clay, *Nat. Prod. Rep.* **2012**, *29*, 1050–1073.
[3] H. G. Smith, M. J. Beech, J. R. Lewandowski, G. L. Challis, M. Jenner, *J. Ind. Microbiol. Biotechnol.* **2021**, *48*, kuab018.
[4] R. S. Gokhale, S. Y. Tsuji, D. E. Cane, C. Khosla, *Science* **1999**, *284*, 482–485.
[5] S. Y. Tsuji, D. E. Cane, C. Khosla, *Biochemistry* **2001**, *40*, 2326–2331.
[6] R. W. Broadhurst, D. Nietlispach, M. P. Wheatcroft, P. F. Leadlay, K. J. Weissman, *Chem. Biol.* **2003**, *10*, 723–731.
[7] T. J. Buchholz, T. W. Geders, F. E. Bartley III, K. A. Reynolds, J. L. Smith, D. H. Sherman, *ACS Chem. Biol.* **2009**, *4*, 41–52.
[8] N. Wu, S. Y. Tsuji, D. E. Cane, C. Khosla, *J. Am. Chem. Soc.* **2001**, *123*, 6465–6474.
[9] N. Wu, D. E. Cane, C. Khosla, *Biochemistry* **2002**, *41*, 5056–5066.
[10] Y. Ogasawara, K. Katayama, A. Minami, M. Otsuka, T. Eguchi, K. Kakinuma, *Chem. Biol.* **2004**, *11*, 79–86.
[11] C. Y. Kim, V. Y. Alekseyev, A. Y. Chen, Y. Tang, D. E. Cane, C. Khosla, *Biochemistry* **2004**, *43*, 13892–13898.
[12] T. Chisuga, A. Nagai, A. Miyanaga, E. Goto, K. Kishikawa, F. Kudo, T. Eguchi, *ACS Chem. Biol.* **2022**, *17*, 198–206.
[13] L. E. N. Quadri, P. H. Weinreb, M. Lei, M. M. Nakano, P. Zuber, C. T. Walsh, *Biochemistry* **1998**, *37*, 1585–1595.
[14] T. Robbins, J. Kapilivsky, D. E. Cane, C. Khosla, *Biochemistry* **2016**, *55*, 4476–4484.
[15] S. Kapur, B. Lowry, S. Yuzawa, S. Kenthirapalan, A. Y. Chen, D. E. Cane, C. Khosla, *Proc. Natl. Acad. Sci. USA* **2012**, *109*, 4110–4115.
[16] D. P. Cogan, K. Zhang, X. Li, S. Li, G. D. Pintilie, S.-H. Roh, C. S. Craik, W. Chiu, C. Khosla, *Science* **2021**, *374*, 729–734.
[17] J. C. Milligan, D. J. Lee, D. R. Jackson, A. J. Schaub, J. Beld, J. F. Barajas, J. J. Hale, R. Luo, M. D. Burkart, S. C. Tsai, *Nat. Chem. Biol.* **2019**, *15*, 669–671.
[18] J. T. Mindrebo, A. Patel, W. E. Kim, T. D. Davis, A. Chen, T. G. Bartholow, J. J. La Clair, J. A. McCammon, J. P. Noel, M. D. Burkart, *Nat. Commun.* **2020**, *11*, 1–15.
[19] C. Nguyen, R. W. Haushalter, D. J. Lee, P. R. L. Markwick, J. Bruegger, G. Caldara-Festin, K. Finzel, D. R. Jackson, F. Ishikawa, B. O'Dowd, J. A. McCammon, S. J. Opella, S. C. Tsai, M. D. Burkart, *Nature* **2014**, *505*, 427–431.
[20] A. Miyanaga, R. Ouchi, F. Ishikawa, E. Goto, G. Tanabe, F. Kudo, T. Eguchi, *J. Am. Chem. Soc.* **2018**, *140*, 7970–7978.
[21] D. Du, Y. Katsuyama, M. Horiuchi, S. Fushinobu, A. Chen, T. D. Davis, M. D. Burkart, Y. Ohnishi, *Nat. Chem. Biol.* **2020**, *16*, 776–782.
[22] A. Miyanaga, S. Iwasawa, Y. Shinohara, F. Kudo, T. Eguchi, *Proc. Natl. Acad. Sci. USA* **2016**, *113*, 1802–1807.
[23] S. Kapur, A. Worthington, Y. Tang, D. E. Cane, M. D. Burkart, C. Khosla, *Bioorg. Med. Chem. Lett.* **2008**, *18*, 3034–3038.
[24] A. Miyanaga, S. Kurihara, T. Chisuga, F. Kudo, T. Eguchi, *ACS Chem. Biol.* **2020**, *15*, 1808–1812.
[25] K. Finzel, D. J. Lee, M. D. Burkart, *ChemBioChem* **2015**, *16*, 528–547.
[26] A. M. Gulick, C. C. Aldrich, *Nat. Prod. Rep.* **2018**, *35*, 1156–1184.
[27] R. W. Haushalter, A. S. Worthington, G. H. Hur, M. D. Burkart, *Bioorg. Med. Chem. Lett.* **2008**, *18*, 3039–3042.
[28] A. Miyanaga, R. Ouchi, F. Kudo, T. Eguchi, *Acta Crystallogr. Sect. F* **2021**, *77*, 294–302.
[29] J. R. Whicher, S. S. Smaga, D. A. Hansen, W. C. Brown, W. H. Gerwick, D. H. Sherman, J. L. Smith, *Chem. Biol.* **2013**, *20*, 1340–1351.
[30] S. Dutta, J. R. Whicher, D. A. Hansen, W. A. Hale, J. A. Chemler, G. R. Congdon, A. R. H. Narayan, K. Håkansson, D. H. Sherman, J. L. Smith, G. Skiniotis, *Nature* **2014**, *510*, 512–517.
[31] S. Kapur, A. Y. Chen, D. E. Cane, C. Khosla, *Proc. Natl. Acad. Sci. USA* **2010**, *107*, 22066–22071.

Manuscript received: April 8, 2022
Revised manuscript received: April 29, 2022
Accepted manuscript online: May 2, 2022
Version of record online: May 16, 2022

© 2022 The Authors. ChemBioChem published by Wiley-VCH GmbH